

Short communication

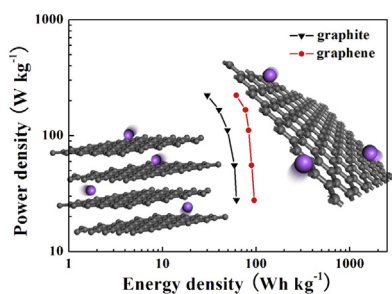
Pre-lithiated graphene nanosheets as negative electrode materials for Li-ion capacitors with high power and energy density

J.J. Ren ^a, L.W. Su ^a, X. Qin ^b, M. Yang ^a, J.P. Wei ^a, Z. Zhou ^{a,*}, P.W. Shen ^a^aTianjin Key Laboratory of Metal and Molecule Based Material Chemistry, Key Laboratory of Advanced Energy Materials Chemistry (Ministry of Education), Institute of New Energy Material Chemistry, Collaborative Innovation Center of Chemical Science and Engineering (Tianjin), Nankai University, Tianjin 300071, China^bDepartment of Chemistry, Tianjin University, Tianjin 300072, China

HIGHLIGHTS

- Pre-lithiated graphene nanosheets are explored for Li-ion capacitors.
- The Li-ion capacitors exhibit high energy and power density at high voltages.
- Pre-lithiated graphene nanosheets are promising for high power Li-ion capacitors.

GRAPHICAL ABSTRACT



ARTICLE INFO

Article history:

Received 27 December 2013
Received in revised form
15 April 2014
Accepted 16 April 2014
Available online 26 April 2014

Keywords:
Lithium ion capacitors
Graphene
Energy density
Power density

ABSTRACT

A Li-ion capacitor (LIC), typically composed of a pre-lithiated negative electrode and an activated-carbon positive electrode, can provide high energy and power density. In this work, we compare the electrochemical performances of pre-lithiated graphene nanosheets and conventional graphite as negative electrode materials for LICs. The LICs employing pre-lithiated graphene nanosheets show a specific capacitance of 168.5 F g^{-1} with 74% capacitance retention at 400 mA g^{-1} after 300 cycles. Moreover, the capacitors deliver a maximum power density of 222.2 W kg^{-1} at an energy density of 61.7 Wh kg^{-1} , operated in the voltage range of 2.0–4.0 V. Therefore, pre-lithiated graphene nanosheets are promising negative electrode materials for high power LICs.

© 2014 Elsevier B.V. All rights reserved.

1. Introduction

With dramatically increasing demand for electric vehicles (EVs) and hybrid EVs in recent years, discovering novel electrochemical energy storage devices with both high power and energy density is a huge challenge. Traditional secondary batteries cannot meet the requirement of high power density [1,2], while electrochemical

double-layer capacitors (EDLCs) with high power density and long cycle life can only provide low energy density [3–5]. Under the circumstances, lithium-ion capacitors (LICs) have emerged and attracted considerable attention. LICs generally utilize pre-lithiated lamellar materials as negative electrodes and high-surface area activated carbon (AC) as positive electrodes [6–9]. In principle, when LICs work in a limited voltage range, anions adsorb/desorbs onto/from the positive electrode surface, and simultaneously Li ions intercalate/de-intercalate into/from the bulk of the negative electrode. Therefore, LICs are amazing energy-storage devices combining the strong points of both EDLCs and secondary batteries

* Corresponding author. Tel.: +86 22 23503623; fax: +86 22 23498941.
E-mail address: zhouchen@nankai.edu.cn (Z. Zhou).

[10]. Unlike EDLCs, the negative electrodes in LICs involve electrochemical reactions of pre-lithiated materials, and then their energy densities are much higher than those of EDLCs. Also, unlike secondary batteries, the positive electrodes of LICs only undergo anion ad/de-sorption on high-surface-area carbon materials and facilitate fast kinetics for charge/discharge processes, which enables higher power densities than those of secondary batteries.

As the Li^+ intercalation/de-intercalation reaction at the negative electrode is much slower than the ad/de-sorption reaction on the surface of the positive electrode, the general performance of LICs will be determined by the negative electrodes [11,12]. Therefore, it is crucial to find an ideal negative electrode material. A variety of materials including graphite, hard carbon and $\text{Li}_4\text{Ti}_5\text{O}_{12}$ (LTO) have been developed as LIC negative electrode materials [13–16], and so far graphite is the most widely used one for LICs. Graphite can offer a relatively flat lithium intercalation/de-intercalation potential between 0.1 and 0.2 V vs. Li/Li^+ and a theoretical capacity of 372 mAh g⁻¹. However, the layered structure of graphite with high crystallinity and anisotropy must impact the rate performance of capacitors under high current densities [13,17]. Similarly, hard carbon was also explored as the negative electrode materials for LICs, and showed good rate capability, which is ascribed to the microstructure of hard carbon. Hard carbon is composed of smaller pieces of graphene layers than graphite, which can contribute to faster ionic diffusion [8]. The good electrochemical performance of hard carbon ultimately comes from the existence of graphene nanosheets (GNSs). Thus, adopting graphene nanosheets to the negative electrode of LICs is highly attractive.

With respect to graphite and hard carbon, graphene possesses some advantages. Graphene, the single layer of carbon atoms in a honeycomb lattice, has high specific surface area, high carrier mobility and outstanding electrical conductivity, providing an ideal platform for the storage and transportation of lithium ions and electrons [18]. As a result, it is a promising material for wide applications, particularly in electronic devices [19–21]. More importantly, the three-dimensional interconnected porous graphene network makes it an ideal material for hybrid capacitors [22,23]. However, graphene, considered as the most potential EDLC material, has scarcely been reported as the negative electrode material for LICs.

As LICs primarily served as power devices, the major criteria for LIC negative electrodes include high capacity, low operation potential and fast charge/discharge capability. Graphene meets these requirements basically. Although the charge/discharge plateaus of graphene are not as flat and low as graphite, which is the problem for graphene's applications as Li ion battery and capacitor electrodes. Fortunately, graphene could supply much larger capacity and boost the energy density of LICs [24–27]. Most importantly, the porous structure and large surface area can afford fast ion transport and rich space for surface/interface electrochemical reactions, which are favorable for supercapacitors.

Herein, we pre-lithiated GNSs and graphite as negative electrode materials for LICs, and compared their performances in cyclic performance, rate capability, as well as energy and power density.

2. Experimental

2.1. Preparation of electrodes

Commercial graphite (Nanshu Hongda, Qingdao) and active carbon (Maxsorb) were used as received. Few-layered GNSs were prepared through exfoliation and chemical reduction of graphite oxide with the assistance of CuBr [25,26,28,29]. The graphite and GNSs were characterized by scanning electron microscope (SEM, FEI Nanosem 430 field-emission gun SEM). The positive electrode

(PE) was composed of AC, acetylene black (AB), and polyvinylidene difluoride (PVDF) with a weight ratio of 80:10:10. Aluminum foil was used as the current collector. For the negative electrode (NE), graphite and graphene were used as the active material, respectively. Negative electrodes were prepared through the same method above except for the ratio of active material, AB, and PVDF (70:20:10). Copper foil was used as the current collector. The average weight of the working electrodes was approximately 3 mg. The electrolyte was 1 mol L⁻¹ LiPF_6 dissolved in a 1:1:1 mixture of ethylene carbonate (EC), ethylene methyl carbonate (EMC) and dimethyl carbonate (DMC). Under the consideration of operating voltage of LICs (2.0–4.0 V), the mass ratio of NE and PE was tailored at 1:2.

2.2. Pre-lithiation of negative electrodes

Pre-lithiated carbon materials can provide low potentials to negative electrodes, increase the open circuit voltage (OCV), and thus enhance the energy density of LICs accordingly [24,27]. As a result, the pre-lithiation is a critical step for LICs. In this work, the pre-lithiation involves the following procedures. Before cycling, the OCV of the cells was about 3.1 V. At first, the cells were discharged (Li^+ intercalation) from its OCV to 0.01 V in Li/carbon cells at a constant current density of 400 mA g⁻¹. In this procedure, graphitic carbon materials tend to form solid electrolyte interface (SEI) films. Therefore, the electrochemical capacity is much higher than that of the following cycles. Next, the cells were charged to OCV at 400 mA g⁻¹ and then discharged/charged in the same way for another two cycles. Fig. 1 shows the charge/discharge curves for the initial three cycles. The capacities became stable in the second and third cycles, and then we set these values as the maximum Li intercalation capacities. Finally, we discharged the electrodes again and controlled the discharge time to insure that 70% of the maximum Li ions were intercalated into the electrodes. The remaining capacity provides the space to Li intercalation/de-intercalation during LIC operation. Therefore, pre-lithiation was successfully accomplished within three discharge/charge cycles and a discharge process in total.

2.3. Electrochemical tests

After pre-lithiation, LICs were assembled in a glove box filled with high-purity argon (H_2O and O_2 < 1 ppm). Galvanostatic charge/discharge tests were performed in the voltage range of 2.0–4.0 V under a LAND-CT2001A instrument at room temperature. The capacitance was calculated according to the corresponding total weight of the active material in both electrodes. Cyclic voltammetry (CV) was performed at a scanning rate of 0.1 mV s⁻¹ between 2.0 and 4.0 V. Electrochemical impedance spectroscopy (EIS) was performed by using an IM6e electrochemical workstation at 25 °C with a frequency range from 10 kHz to 100 mHz and an alternating current signal with an amplitude of 5 mV as the perturbation.

3. Results and discussion

3.1. Microstructure characterizations

The SEM images of graphite and graphene are displayed in Fig. 2. The graphite sample has thick and lamellar morphology while the graphene sample shows an irregular shape with cross-linked nanosheets.

Since the intercalation/de-intercalation of Li ions is strongly affected by pore size distribution [30–32], we compared the pore size distributions of graphite and GNSs (Fig. 3). There is significant difference between those two curves. GNSs present a unimodal

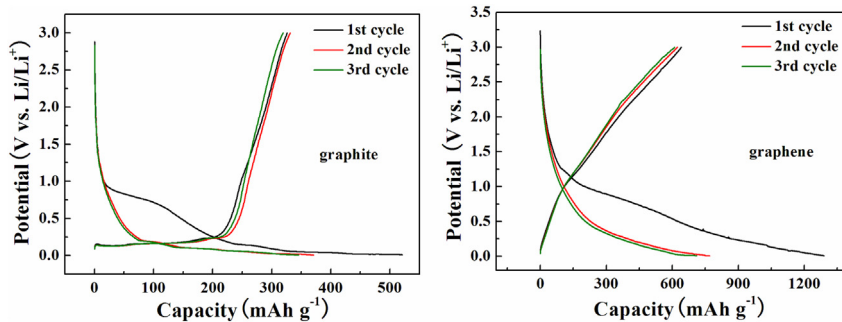


Fig. 1. Galvanostatic charge/discharge curves of Li/graphite 2-electrode cells at a constant current density of 400 mA g^{-1} between the OCV and 0.01 V vs. Li^+/Li .

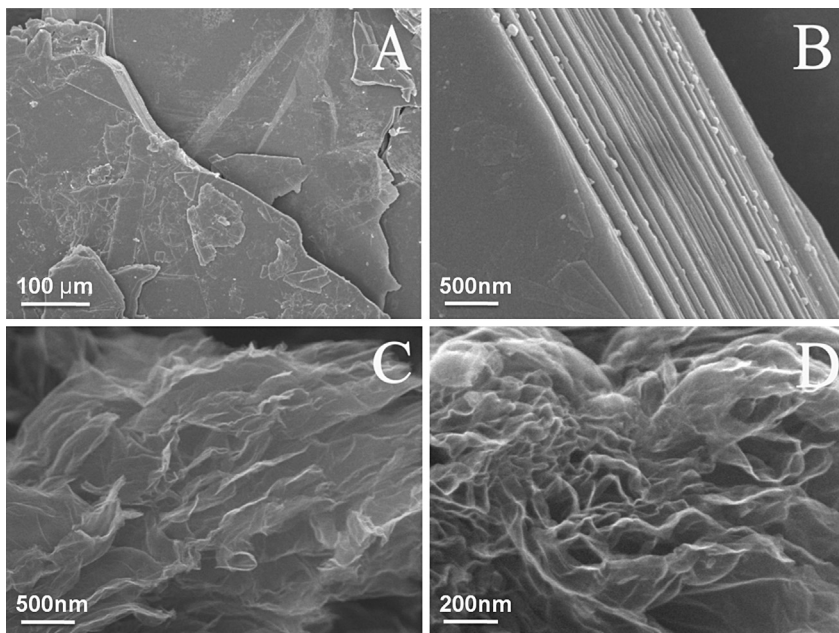


Fig. 2. SEM images of graphite (A, B) and graphene (C, D).

wide pore size distribution with average pore diameter around 2.5 nm . It proved the microporous character of GNSs; moreover, the significant contribution of mesopores cannot be neglected. Both pores play an important role in charge accumulation; micropores are responsible for charge storage and ion intercalation/de-intercalation, whereas mesopores function as channels for ion transport from the electrolyte to electrode interface. They can reduce the charge transfer impedance and enhance Li^+ diffusion, which can be proved by the following EIS tests. By contrary, the pore size distribution of graphite is almost flat, indicating no pore distribution basically. The reason is that GNSs are composed of curly layers while graphite has thick and lamellar morphology, which can be confirmed in SEM images (Fig. 2).

3.2. Electrochemical performances

The specific capacitances of the electrodes were measured by means of galvanostatic charge/discharge tests. Fig. 4(a) shows the cycle performance of the LICs employing AC (positive electrode) and pre-lithiated graphite and graphene (negative electrode), respectively. All the capacitors were tested in the voltage window of $2.0\text{--}4.0 \text{ V}$ at a constant current density of 400 mA g^{-1} . As shown in Fig. 4(a), the initial capacitance is 180.7 F g^{-1} for graphite and

228 F g^{-1} for graphene. In the subsequent cycles, it is found that the capacitance of graphene exhibited a considerable stability with high capacitance retention of $\sim 74\%$ while graphite had the retention of about 38% after 300 cycles. It indicates that the microstructure of GNSs is more stable after long term cycling. Fig. 4(b) shows the cycle performances of LICs at successively increased

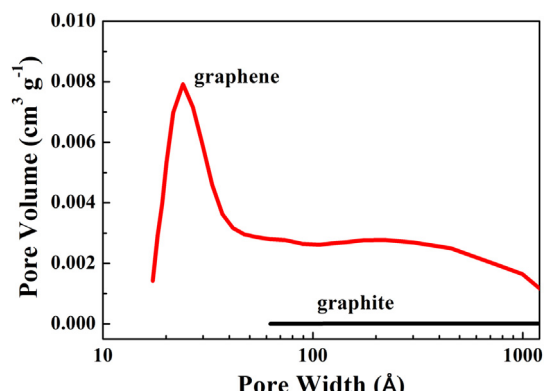


Fig. 3. Pore size distributions of graphite and graphene.

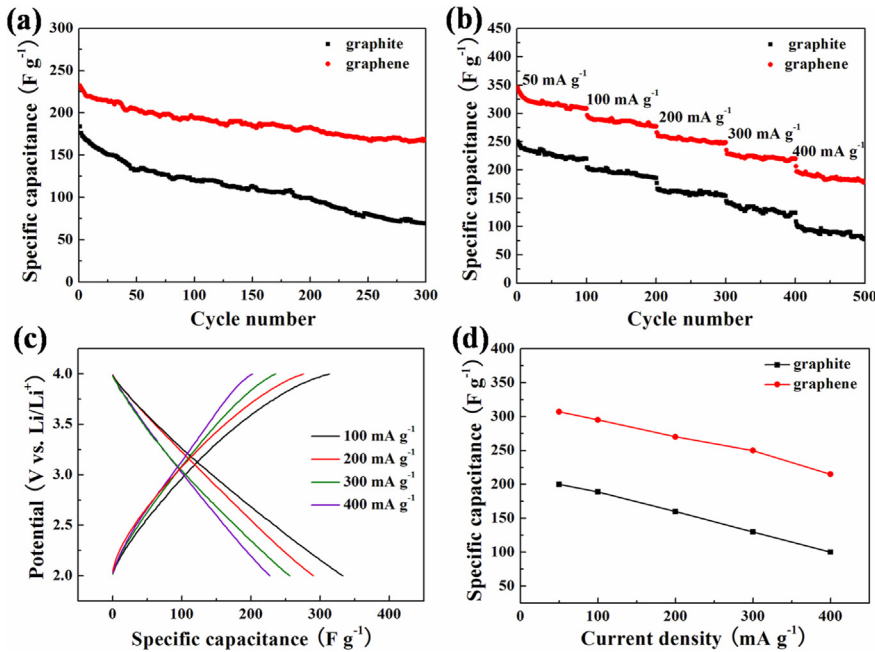


Fig. 4. (a) Cycling performance of the LICs employing pre-lithiated graphite and graphene as negative electrode in the voltage window of 2.0–4.0 V at a constant current density of 400 mA g^{-1} . (b) Cycling performance of the LICs employing pre-lithiated graphite and graphene as negative electrode in the voltage window of 2.0–4.0 V at successively increased current densities. (c) Initial charge/discharge curves of the LICs employing pre-lithiated graphene as negative electrode at various current densities. (d) Corresponding specific capacitances of the LICs employing pre-lithiated graphite and graphene as negative electrode at different current densities.

current densities from 50 mA g^{-1} to 400 mA g^{-1} . During the initial 100 cycles at 50 mA g^{-1} , graphene shows a capacitance of 327 F g^{-1} , with only 6% of capacitance loss after 100 cycles. In the following cycles, graphene delivers a capacitance of 291 and 268 F g^{-1} at 100 mA g^{-1} and 200 mA g^{-1} , respectively. After 500 continuous cycles at successive increased current densities, the retained capacitance for graphene is 203 F g^{-1} with capacitance retention of 62.1%, which is higher than that of graphite (with capacitance retention of 45%). The better rate capability and cycle performance of pre-lithiated graphene could be attributed to the disordered microstructure consisting of cross-linked graphene nanosheets, which may lead to fast Li^+ diffusion under high-rate charge/discharge conditions.

Fig. 4(c) shows the charge/discharge curves of LICs employing pre-lithiated graphene at different current densities. The curves appear no platform since the cell mainly exhibits capacitive behavior. The specific capacitance of the electrode can be calculated according to the equation: $C = It/\Delta V$, where I is the discharge current (A), t is the discharge time (s), m is the mass of active material (g), and ΔV is the potential window (V) of the discharge process.

The calculated specific capacitances of graphene for the first discharge are 346.5, 292, 254 and 230.5 F g^{-1} at different discharge current densities of 100, 200, 300 and 400 mA g^{-1} , respectively. Moreover, Fig. 4(d) shows the specific capacitance of LICs employing pre-lithiated graphene and graphite at increased current densities. As shown in Fig. 4(d), LICs employing pre-lithiated graphene show higher specific capacitance than graphite at any current density. The comparison of those two materials reveals that our graphene-based LICs exhibit good cyclic stability and rate capability during repetitive charge/discharge cycles.

Fig. 5 shows the CV curves of the cells assembled with pre-lithiated graphene nanosheets and graphite electrodes in the initial four cycles. In the voltage range from 2.0 to 4.0 V, the CV curve of graphene manifests a nearly rectangular shape indicating an ideal capacitive behavior. With the cycle going on, the curves change slightly. Because of the solution resistance, the effective diffusion coefficient is quite small and thus the establishment of adsorption equilibrium in micropores/mesopores is a very slow process. Compared with graphene, the CV curve of graphite becomes distorted from a rectangle. The nearly mirror symmetrical

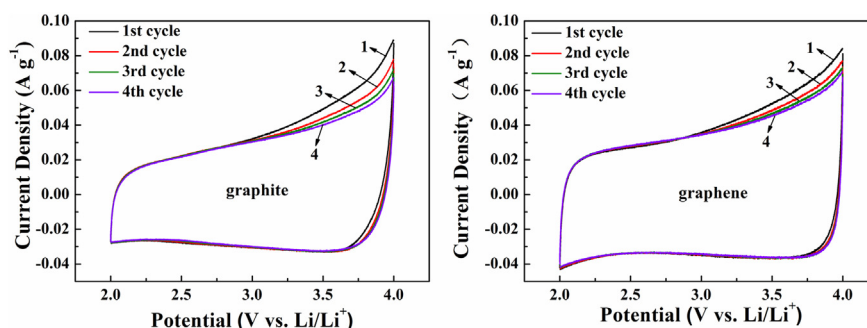


Fig. 5. CV curves of the LICs employing activated carbon (positive electrode) and pre-lithiated graphite and graphene (negative electrode) materials in the initial four cycles.

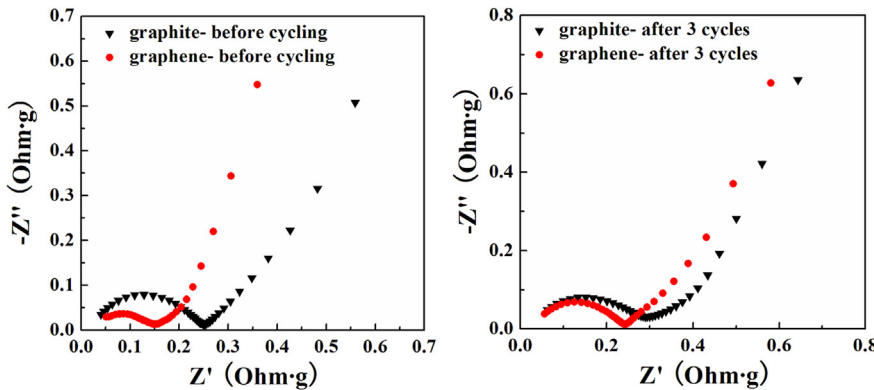


Fig. 6. Nyquist plots of the LICs employing activated carbon (positive electrode) and pre-lithiated graphite and graphene (negative electrode), before cycling and after 3 cycles.

CV shape is indicative of good charge propagation within the graphene electrodes.

EIS is effective for evaluation of the electron conductivity and Li^+ diffusion process of materials. EIS can reflect the information of entire LICs cells, including the positive and negative electrodes. The Nyquist plots of graphite and graphene electrodes at different stages are demonstrated in Fig. 6. The high-frequency semicircle is assigned to charge transfer impedance of the electrode/electrolyte interface [33], reflecting two processes: anions adsorb/desorb onto/from the surface of positive electrodes and Li ions pass through from the electrolyte to the surface of negative electrodes. The line corresponds to Li^+ diffusion process inside the electrodes, indicating Li ions intercalate/de-intercalate in the bulk of the negative electrode. In comparison with graphite, graphene electrodes have a smaller impedance and superior Li^+ diffusion process before cycling and after 3 cycles, which can be ascribed to the excellent conductivity of graphene. After 3 cycles, two obvious characteristics of the Nyquist plots can be observed and the semicircle becomes more obvious, indicating that the charge-transfer resistance increases with cycling. In addition, both the real and imaginary parts of impedance for the third cycle are larger than that of the first cycle, which is attributed to the increased diffusion and migration pathways of electrolyte ions during the charge/discharge process.

The Ragone plots for the capacitors are illustrated in Fig. 7, obtained by calculating the energy and power density from the galvanostatic discharge characteristics at current densities from 50 mA g^{-1} to 400 mA g^{-1} . The total mass of active materials in both electrodes is considered for the calculation. Note that with the increase of current density from 50 mA h^{-1} to 400 mA h^{-1} , LICs

employing pre-lithiated graphene show greater energy density than those employing pre-lithiated graphite at roughly the same power density. Moreover, the pre-lithiated graphene LICs could exhibit a maximum power density of 222.2 W kg^{-1} with an energy density of 61.7 Wh kg^{-1} at a current density of 400 mA h g^{-1} . As the LIC will primarily serve as a power device, it is expected to quickly charge/discharge in a short time. Hence, pre-lithiated graphene nanosheets are more suitable as negative electrode materials for high power LICs.

4. Conclusions

The electrochemical characteristics of two kinds of carbon materials (pre-lithiated graphite and graphene) have been evaluated as negative electrode for Li-ion capacitors. The pre-lithiated graphene shows excellent specific capacitance, cyclic stability and rate capability, as the negative electrode material for LICs, compared with pre-lithiated graphite. Moreover, the LICs employing pre-lithiated graphene nanosheets delivered a maximum power density of 222.2 W kg^{-1} at an energy density of 61.7 Wh kg^{-1} , operated in the voltage range of $2.0\text{--}4.0 \text{ V}$. Its better electrochemical performances are mainly attributed to the microstructure consisting of cross-linked graphene nanosheets with high specific surface areas and rich pores. Therefore, pre-lithiated graphene nanosheets are more suitable as negative electrode materials for high power Li-ion capacitors.

Acknowledgments

This work was supported by NSFC (21273118) and MOE Innovation Team (IRT13022) in China.

References

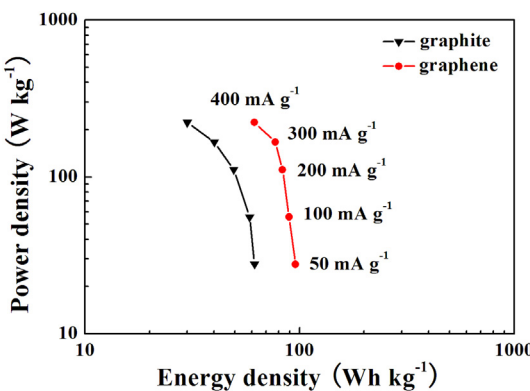


Fig. 7. Ragone plots for the LICs employing activated carbon (positive electrode) and pre-lithiated graphite and graphene (negative electrode).

- [1] J.B. Goodenough, K.S. Park, *J. Am. Chem. Soc.* 135 (2013) 1167–1176.
- [2] H.-K. Song, K.T. Lee, M.G. Kim, L.F. Nazar, J. Cho, *Adv. Funct. Mater.* 20 (2010) 3818–3834.
- [3] P. Sharma, T.S. Bhatti, *Energ. Convers. Manag.* 51 (2010) 2901–2912.
- [4] M. Inagaki, H. Konno, O. Tanaike, *J. Power Sources* 195 (2010) 7880–7903.
- [5] R. Kötz, M. Carlen, *Electrochim. Acta* 45 (2000) 2483–2498.
- [6] N. Omar, M. Daoud, O. Hegazy, M. Al Sakka, T. Coosemans, P. Van den Bossche, J. Van Mierlo, *Electrochim. Acta* 86 (2012) 305–315.
- [7] N. Böckenfeld, R.S. Kühnel, S. Passerini, M. Winter, A. Balducci, *J. Power Sources* 196 (2011) 4136–4142.
- [8] J.-H. Kim, J.-S. Kim, Y.-G. Lim, J.-G. Lee, Y.-J. Kim, *J. Power Sources* 196 (2011) 10490–10495.
- [9] S.R. Sivakkumar, A.G. Pandolfo, *Electrochim. Acta* 65 (2012) 280–287.
- [10] W.H. Shin, H.M. Jeong, B.G. Kim, J.K. Kang, J.W. Choi, *Nano Lett.* 12 (2012) 2283–2288.
- [11] C. Decaux, G. Lota, E. Raymundo-Piñero, E. Frackowiak, F. Béguin, *Electrochim. Acta* 86 (2012) 282–286.

- [12] B.Z. Jang, C. Liu, D. Neff, Z. Yu, M.C. Wang, W. Xiong, A. Zhamu, *Nano Lett.* 11 (2011) 3785–3791.
- [13] V. Khomenko, E. Raymundo-Pinero, F. Béguin, *J. Power Sources* 177 (2008) 643–651.
- [14] K. Naoi, *Fuel Cells* 10 (2010) 825–833.
- [15] P. Simon, Y. Gogotsi, *Nat. Mater.* 7 (2008) 845–854.
- [16] K. Naoi, S. Ishimoto, J.-i. Miyamoto, W. Naoi, *Energy Environ. Sci.* 5 (2012) 9363.
- [17] S.R. Sivakkumar, J.Y. Nerkar, A.G. Pandolfo, *Electrochim. Acta* 55 (2010) 3330–3335.
- [18] N.O. Weiss, H. Zhou, L. Liao, Y. Liu, S. Jiang, Y. Huang, X. Duan, *Adv. Mater.* 24 (2012) 5782–5825.
- [19] J. Chen, C. Li, G. Shi, *J. Phys. Chem. Lett.* 4 (2013) 1244–1253.
- [20] Q. Tang, Z. Zhou, Z.F. Chen, *Nanoscale* 5 (2013) 4541–4583.
- [21] Q. Tang, Z. Zhou, *Prog. Mater. Sci.* 58 (2013) 1244–1315.
- [22] J.R. Miller, R.A. Outlaw, B.C. Holloway, *Electrochim. Acta* 56 (2011) 10443–10449.
- [23] K. Leng, F. Zhang, L. Zhang, T. Zhang, Y. Wu, Y. Lu, Y. Huang, Y. Chen, *Nano Res.* 6 (2013) 581–592.
- [24] Z.S. Wu, W. Ren, L. Xu, F. Li, H.M. Cheng, *ACS Nano* 5 (2011) 5463–5471.
- [25] P. Lian, X. Zhu, S. Liang, Z. Li, W. Yang, H. Wang, *Electrochim. Acta* 55 (2010) 3909–3914.
- [26] E. Yoo, J. Kim, E. Hosono, H.S. Zhou, T. Kudo, I. Honma, *Nano Lett.* 8 (2008) 2277–2282.
- [27] P. Guo, H. Song, X. Chen, *Electrochim. Commun.* 11 (2009) 1320–1324.
- [28] G. Wang, X. Shen, J. Yao, J. Park, *Carbon* 47 (2009) 2049–2053.
- [29] L. Wang, Q. Tang, X. Li, X. Qin, *Mater. Lett.* 106 (2013) 356–359.
- [30] L.J. Cote, R. Cruz-Silva, J. Huang, *J. Am. Chem. Soc.* 131 (2009) 11027–11032.
- [31] Y. Zhu, S. Murali, W. Cai, X. Li, J.W. Suk, J.R. Potts, R.S. Ruoff, *Adv. Mater.* 22 (2010) 3906–3924.
- [32] W.S. Hummers, R.E. Offeman, *J. Am. Chem. Soc.* 80 (1958) 1339–1340.
- [33] J. Gamby, P.L. Taberna, P. Simon, J.F. Fauvarque, M. Chesneau, *J. Power Sources* 101 (2001) 109–116.